

# Numerical simulation of the motion of a micropolar Casson fluid through a porous medium over a stretching surface

<sup>1</sup>N.T. Eldabe, <sup>2</sup>G.M. Moatimid, <sup>3</sup>A.A. ElShekhiy, <sup>4</sup>Naglaa F.Aballah

<sup>1,2,4</sup>Department of Mathematics, Faculty of Education, Ain Shams University, Roxy, Heliopolis, Cairo, Egypt.

<sup>3</sup>Mathematics Department, Faculty of Science, Imam Abdulrahman Bin Faisal University, Al-Dammam, Kingdom of Saudi Arabia.

## Abstract

The present study examines the motion of a micropolar non-Newtonian Casson fluid through a porous medium over a stretching surface. The system is pervaded by an external uniform magnetic field. The heat transfer and heat generation are taken into consideration. The problem is modulated mathematically by a system of nonlinear partial differential equations which describe the equations of continuity, momentum and energy. Suitable similarity solutions are utilized to transform the system of equation to ordinary nonlinear differential equations. In accordance with the appropriate boundary conditions, are numerically solved by means of the finite difference technique. Also, the system is solved by using multistep differential transform method. The effects of the various physical parameters, of the problem at hand, are illustrated through a set of diagrams.

**Keywords:** Micropolar Casson fluid; Porous medium; Multi-step differential transform method (Ms-DTM); Finite difference method (FDM).

## Nomenclature:

$T_{\infty}$ .	Temperature at infinity	$h_a$	The Hartmann number,
$T_w$ .	The temperature at the stretched plane	$D_a$	The Darcy number,
$B_0$	A uniform magnetic field	$S$	The porous medium shape factor parameter
$N$	The microrotation vector	$P_r$	The Prandtl number
$\gamma$	The electric conductivity	$E_c$	The Eckert number
$K$	Dimensionless velocity ratio parameter	$B$	The dimensionless heat generation/ absorption parameter.
$n$	Boundary concentration parameter of fluid	$\mu$	The spin gradient viscosity
$c_p$	The specific heat at constant pressure	$k$	The thermal diffusivity
$Ka$	The Darcy permeability	$\rho$	The fluid density

## 1 Introduction

The theory of micropolar fluid has been a field of very active research because it takes into consideration the microscopic influences arising from the local structure and micro motions of the fluid elements. The theory is expected to provide a mathematical model, which can be utilized to describe the behavior of non-Newtonian fluids such as liquid crystals, polymeric fluids, paints, animal blood, Ferro liquids, colloidal fluids, etc. The concept of simple micro fluids to characterize concentrated suspensions of neutrally buoyant deformable particles in a viscous fluid where the individuality of substructures affects the physical outcome of the flow was discussed by Eringen [1]. Such fluids models can be used to rheological describe normal human blood, polymeric suspensions, etc. Also, they have found applications in physiological and engineering problems. Ali and Hayat [2] carried out a study of peristaltic motion of an incompressible micropolar fluid in an asymmetric channel, the flow analysis has been developed for low Reynolds number and long wavelength case. Also, they compared the results for micropolar fluid with those for Newtonian fluid. The influences of thermal radiation on MHD axisymmetric stagnation point flow and heat transfer of a micropolar fluid over a shrinking sheet was discussed by Shahzad, et al [3]. In another paper, Eldabe, et al. [4] studied magnetohydrodynamic (MHD) peristaltic flow with heat and mass transfer of micropolar biviscosity fluid through a porous medium between two co-Axial tubes. They obtained the effects of physical parameters on Nusselt number and Sherwood number. Nazeer et al [5] discussed the numerical simulation of MHD flow of micropolar fluid inside a porous inclined cavity with uniform and non-uniform heated bottom wall. Free convective micropolar fluid flow and heat transfer over a shrinking sheet with heat source was delineated by Mishra et al [6]. For more details and thermos physical properties of micropolar fluid see ref [7-12].

Flow through a porous medium has several practical applications especially in geophysical fluid dynamics. Examples of natural porous media are sandstone, beach sand, the human lung, limestone, bile duct and gall bladder with stones in small blood vessels. Eldabe, et al. [13] constructed heat and mass transfer of magnetohydrodynamic pulsatile flow of Casson fluid with couple stress through porous medium. Mekheimer [14] delineated the nonlinear peristaltic transport through a porous medium in an inclined planar channel. Zueco and Ahmed [15] discussed the combined heat and mass transfer by mixed convection MHD flow along a porous plate with chemical reaction in presence of heat source, and they found that the flow velocity, the fluid temperature, and the induced magnetic field decrease with the increase in the destructive chemical reaction. In another paper, Moatimid, et al. [16], scrutinized the influence of partial slip on peristaltic flow of a Sisko fluid with mild stenosis through a porous medium and found that the Darcy's coefficient of the fluid restrains the velocity.

The Casson fluid model is used to predict blood flow in arteries at very low shear rate. Also, it utilized in perception flow behavior of pigment oil suspensions of the printing ink type. The shear stress-shear rate relation given by Casson satisfactorily describes the properties of many polymers over a wide range of shear rates [17]. A numerical investigation of micropolar Casson fluid over a stretching sheet with internal heating was reported by Mehmoo et al. [18]. Impact of inclined magnetic field on micropolar Casson fluid. Further, the influence of inclined magnetic field on micropolar Casson fluid using Keller box algorithm was studied by Iqbal et al. [19].

The study of stagnation point flow was pioneered by Hiemenz [20]. A flow can be stagnated by a solid wall, a free stagnation point or a line can exist in the interior of the fluid domain Shateyi and

Makinde [21]. Bhattacharyya et al. [22] scrutinized the effects of partial slip on steady boundary layer stagnation-point flow of an incompressible fluid and heat transfer towards a shrinking sheet. The relevance of this study attracted Motsa et al. [23] to formulate mathematical equation governing Maxwell fluid for two-dimensional stagnation flow towards a shrinking sheet and analyzed the flow behavior extensively using similarity variables together with successive linearization method. Javed and Ghaffari [24] addressed the numerical study of non-Newtonian Maxwell fluid in the region of oblique stagnation point flow over a stretching sheet. Mustafa et al [25] scrutinized the heat transfer in MHD stagnation point flow of a ferrofluid over a stretchable rotating disk. Further, the heat transfer analysis of unsteady oblique stagnation point flow of elastico-viscous fluid due to sinusoidal wall temperature over an oscillating-stretching surface: A numerical approach was deliberated by Ghaffari et al [26].

Internal energy generation can be explained as a scientific method of generating heat energy within a body by a chemical, electrical or nuclear process. Natural convection induced by internal heat generation is a common phenomenon in nature. Example includes motion in the atmosphere where heat is generated by absorption of sunlight [27]. Crepeau and Clarksean [28] carried out a similarity solution for a fluid with an exponential decaying heat generation term and a constant temperature vertical plate under the assumption that the fluid under consideration has an internal volumetric heat generation. In many situations, there may be appreciable temperature difference between the surface and the ambient fluid. This necessitates the consideration of temperature dependent heat sources that may exert a strong influence on the heat transfer characteristics (see Salem, et al. [29]). In another paper, El-Aziz and Salem [30] has stated that exact modeling of internal heat generation/absorption is quite difficult and argued that some simple mathematical models can express its average behavior for most physical situations. Muhammad et al [31] debated the Rotating Flow of Magneto Hydrodynamic Carbon Nanotubes over a Stretching Sheet with the Impact of Non-Linear Thermal Radiation and Heat Generation/Absorption. For more details and application in this direction see ref [32-37].

The micropolar casson fluid problems with heat generation and porous medium are modeled by a set of coupled non-linear partial differential equations, combined with the geometrical complexity of these problems which makes analytical or closed form solutions virtually impossible to obtain. Therefore a substantial amount of research work has been invested in order to obtain satisfactory solutions. The present investigation uses the FDM as well as the Ms-DTM methods to overcome the highly nonlinear terms that appear in micropolar Casson fluid models. The Ms-DTM method accelerates the convergence of the series solution over large region and yields a series solution, this series will be truncated due to the required accuracy of solutions. This modified technique is verified through illustrative examples of non-chaotic or chaotic systems by Odibat, et al, [38]. Further, to get more accurate results Zait, et al. [39], studied the statistical measures approximations for the Gaussian part of the stochastic nonlinear damped Duffing oscillator solution process under the application of Wiener Hermite expansion linked by the multi-step differential transformed method. Finite difference method is proposed by Courant, et al [40] in 1928. Finite-difference methods (FDM) are numerical methods that give a solution to the differential equations by approximating them with difference equations (see Refs. [41]). In another paper, Thomee [42] introduced a short history of numerical analysis of partial differential equations to finite differences and finite elements.

The aim of the present work is to extend the work of Shahzad et al [23], to include the motion of micropolar Casson fluid in a porous medium. A detailed comparison between Ms-DTM and FDM methods is made to show an agreement between them. Moreover concluding remarks are summarized in the last section.

## 2 Mathematical formulations

It is convenient to use the Cartesian coordinates in two-dimensions, say  $(x, y)$ . The temperature at the stretched plane  $y = 0$  is taken as  $T_w$ . Meanwhile, the temperature at  $\infty$  is referred by  $T_\infty$  (see Fig 1). A uniform magnetic field  $B_0$  is acted upon the negative direction of the  $x - axis$ .

The constituting equations of continuity, conservation momentum, angular momentum and energy with compressibility conditions are summarized as [15, 20, 29]:

Continuity equation:

$$\frac{\partial u}{\partial x} + \frac{\partial v}{\partial y} = 0, \quad (1)$$

The conservation momentum yields:

$$u \frac{\partial u}{\partial x} + v \frac{\partial u}{\partial y} = U \frac{\partial U}{\partial x} + v \left( 1 + \frac{k}{\mu} + \frac{1}{\beta} \right) \frac{\partial^2 u}{\partial y^2} + \frac{k}{\rho} \frac{\partial N}{\partial y} + \left( \frac{\sigma B_0^2}{\rho} + \frac{\mu}{\rho K_d} \right) (U - u), \quad (2)$$

The angular momentum equation:

$$\rho \left( u \frac{\partial N}{\partial x} + v \frac{\partial N}{\partial y} \right) = \mu \left( 1 + \frac{k}{2} \right) \frac{\partial^2 N}{\partial y^2} - \mu k \left( 2N + \frac{\partial u}{\partial y} \right), \quad (3)$$

Finally, the energy equation given:

$$u \frac{\partial T}{\partial x} + v \frac{\partial T}{\partial y} = \alpha \frac{\partial^2 T}{\partial x^2} (U - u)^2 + \frac{v}{c_p} \left( 1 + \frac{1}{\beta} \right) \left( \frac{\partial u}{\partial y} \right)^2 + \frac{Q}{\rho c_p} (T - T_\infty). \quad (4)$$

It is convenient to consider the appropriate boundary condition as follows [3]:

$$u = ax, v = 0, N = -n \frac{\partial u}{\partial y}, T = T_w, \text{ at } y = 0, \quad (5)$$

$$u(x) = bx, N \rightarrow 0, T \rightarrow T_\infty, \text{ as } y \rightarrow \infty. \quad (6)$$

where  $\mu$  is the dynamics viscosity,  $k$  is the thermal diffusivity,  $\rho$  is the fluid density,  $N$  is the microrotation vector (or angular velocity),  $\mu$  is the spin gradient viscosity,  $\gamma$  is the electric conductivity,  $K$  is the dimensionless velocity ratio parameter,  $B_0$  is the strength of magnetic field,  $n$  is the boundary concentration parameter of fluid,  $c_p$  is the specific heat at constant pressure,  $K_d$  is the Darcy permeability.

To simplify the analysis of solutions for the above equations, It is convenient to consider the following procedure:

- The similarity is useful to convert the partial differential equation to ordinary differential equation
- The dimensionless quantities are very important to provide the characteristic dimensionless number with its useful.

$$\eta = \left( \frac{a}{v} \right)^{\frac{1}{2}} y, u = ax f'(\eta), v = -(av)^{\frac{1}{2}} f'(\eta), N = ax \left( \frac{a}{v} \right)^{\frac{1}{2}} g(\eta). \quad (7)$$

and

$$T = \Delta T \theta(\eta) + T_\infty \text{ or } \theta = \frac{T - T_\infty}{T_w - T_\infty}. \quad (8)$$

Thus, equations ((2)-(4)) becomes

Momentum yields:

$$\left(1 + \frac{k}{\mu} + \frac{1}{\beta}\right) f'''' + f f'' - f'^2 + K g' + (h_a^2 + S^2)(C - f'^2) = 0. \quad (9)$$

The angular momentum equation:

$$\left(1 + \frac{K}{2}\right) g'' + f g' - f' g - K(2g + f'') = 0. \quad (10)$$

Finally, the energy equation given:

$$\frac{1}{P_r} \theta'' + f \theta' + E_c \left(1 + \frac{1}{\beta}\right) f''^2 + h_a^2 E_c (C - f'^2 + B\theta) = 0. \quad (11)$$

The corresponding boundary conditions become:

$$f(0) = 0, f'(0) = 1, f'(\infty) = C, \quad (12)$$

$$\theta(0) = 1, \theta(\infty) = 0, g(0) - n f''(0), g(\infty) = 0. \quad (13)$$

Where  $h_a^2 = \frac{\sigma_e B_0^2}{\rho a}$  is the Hartmann number,  $D_a = \frac{a K d}{\nu}$  is the Darcy number,  $S = \frac{1}{\sqrt{D_a}}$  is the porous

medium shape factor parameter,  $P_r = \frac{\mu c_p}{k_0}$  is the Prandtl number,  $E_c = \frac{U^2}{\Delta T c_p}$  is the Eckert number and

$B = \frac{Q}{a \rho c_p}$  is the dimensionless heat generation/absorption parameter.

### 3 Multi-step differential equation method

Using similar arguments as given by [38]. The equations of motion as mentioned in (9-11) with the appropriate boundary conditions (12-13) are transformed to

Conversation of momentum yields:

$$\begin{aligned} & \left(1 + \frac{k}{\mu} + \frac{1}{\beta}\right) (k+1)(k+2)(k+3)F(k+3) + K(k+1)G(k+1) - (h_a^2 + S^2)(k+1)F(k+1) + \\ & [(h_a^2 + S^2)c + c^2]\delta[k] + \sum_{r=0}^k (r+1)(r+2)F(r+2)F(k-r) - \sum_{r=0}^k (r+1)(r+2)F(r+ \\ & 1)F(k-r+1), \end{aligned} \quad (14)$$

The angular momentum equation gives:

$$(1+K)(k+1)(k+2)G(k+1) - K(2G[k] + (k+1)(k+2)F(k+2)) + \sum_{r=0}^k (r+1)[G(r+1)F(k-r) - F(r+1)G(k-r)] = 0, \quad (15)$$

Finally, the energy equation is given by:

$$\begin{aligned} & \frac{1}{P_r} (k+1)(k+2)\theta(k+2) + B\theta[k] - 2h_a^2 E_c C(k+1)F(k+1) + P_r h^2 E_c C^2 \delta[k] + \sum_{r=0}^k (r+ \\ & 1)\theta(r+1)F(k-r) + \left(1 + \frac{1}{\beta}\right) \sum_{r=0}^k (r+1)(r+2)F(r+2)(k-r+1)(k-r+2)F(k-r+2) + \\ & h_a^2 E_c \sum_{r=0}^k (r+1)F(r+1)(k-r+1)F(k-r+1) = 0, \end{aligned} \quad (16)$$

where  $F[k], G[k]$  and  $\theta[k]$  are the differential transformation functions of  $f(\eta), g(\eta)$  and  $\theta(\eta)$  respectively. The differential transform of the related boundary conditions are given by respectively.

The differential transform of the associated boundary conditions are given by

$$F[0] = 0, F[1] = 1, G[0] = -2nF[2], \theta[0] = 1,$$

$$\sum_{r=0}^k F_k[\eta_\infty]^k = C, \sum_{r=0}^k G_k[\eta_\infty]^k = 0, \sum_{r=0}^k \theta_k[\eta_\infty]^k = 0. \quad (17)$$

By substituting from Eq. (17) in Eqs. (14-16), we obtain series of solutions to the velocity, microrotation and temperature distributions. They are achieved with the aid of MATHEMATICA10 software.

## 4 Finite difference method

The implicit finite-difference method is used to solve Eqs. (see refs. [42]). (9)–(11) subject to the boundary conditions of eq. (12-13). This scheme is unconditionally stable and gives a better accuracy. We use a FDM to solve a system of differential Eqs. (9) - (11). We reduce the order of these equations with the help of the substitution  $q = f'$ .

$$\left(1 + \frac{k}{\mu} + \frac{1}{\beta}\right) q'' + f q' - q^2 + K g' + (h_a^2 + S^2)(C - q^2) = 0. \quad (18)$$

$$\left(1 + \frac{K}{2}\right) g'' + f g' - q g - K(2g + q') = 0. \quad (19)$$

$$\frac{1}{P_r} \theta'' + f \theta' + E_c \left(1 + \frac{1}{\beta}\right) q'^2 + h_a^2 E_c (C - q^2 + B\theta) = 0. \quad (20)$$

Subject to the boundary conditions (10) which become

$$f(0) = 0, q(0) = 1, q(\infty) = C, \theta(0) = 1, g(0) = -nq'(0), g(\infty) = 0. \quad (21)$$

The system of nonlinear differential Eqs. (18) and (20) are solved under the boundary conditions which are given by Equation (21).

$$\left(1 + \frac{k}{\mu} + \frac{1}{\beta}\right) \left[\frac{q_{i-1} - 2q_i + q_{i+1}}{\Delta^2}\right] + (h_a^2 + S^2)(C - \bar{q}_i q_i) + \bar{f}_i \left[\frac{q_{i+1} - q_{i-1}}{2\Delta}\right] - \bar{q}_i q_i + K \left[\frac{g_{i+1} - g_{i-1}}{2\Delta}\right] = 0. \quad (22)$$

$$\left(1 + \frac{K}{2}\right) \left[\frac{g_{i-1} - 2g_i + g_{i+1}}{\Delta^2}\right] + \bar{f}_i \left[\frac{g_{i+1} - g_{i-1}}{2\Delta}\right] - \bar{q}_i g_i - K \left(2g_i + \left[\frac{q_{i+1} - q_{i-1}}{2\Delta}\right]\right) = 0. \quad (23)$$

$$\frac{1}{P_r} \left[\frac{\theta_{i-1} - 2\theta_i + \theta_{i+1}}{\Delta^2}\right] + \bar{f}_i \left[\frac{\theta_{i+1} - \theta_{i-1}}{2\Delta}\right] + E_c \left(1 + \frac{1}{\beta}\right) \left[\frac{q_{i+1} - q_{i-1}}{2\Delta}\right]^2 + h_a^2 E_c (C - \bar{q}_i q_i + B\theta_i) = 0. \quad (24)$$

## 5 Results and Discussion

This section is devoted to discuss the solutions by the above two methods, Firstly, the multi-step differential equation and secondly, finite difference method. After that a comparison between these two methods is computed, and offered in the following subsection.

### 5.1 Comparison between two numerical methods

The present investigation is used the FDM as well as the Ms-DTM methods. A detailed comparison between those methods was made to show agreement between them through figures 1-3 and table 1 as follows:

It is noticed from Figs. 2-4. that the solutions of velocity, microrotation and temperature profiles evaluated by using DTM accept the behavior of numerical solution till a point Q, and then it diverges. So we utilize the Ms-DTM and FDM methods, those provide the solutions in terms of convergent series over a sequence of subintervals. In fact, our results indicate a close agreement between the finite difference and Multi-step differential transform methods as shown in Figs. 2-4 and table 1. Thereafter, the influences of physical parameters (the Casson parameter  $\beta$ , the Hartmann number  $ha$ ; the porous medium shape factor parameter  $S$  and the dimensionless heat generation/absorption parameter  $B$ ) on the velocity  $f(\eta)$ ; microrotation  $g(\eta)$  and temperature profile  $\theta(\eta)$  by using Ms-DTM are illustrated through Figs. 5-14. At what follows, the numerical estimations concern with the method of Ms-DTM, the target now is find the influences of various parameter for the above distributions.

#### 5.1.1 For the velocity profile

**Figs. 5-7** are displayed to visualize the effect of various parameter on velocity profile. The calculation shows the following results.

- It's seen from **Fig. 5** and **6**. that an increase in Casson parameter and Hartmann number  $h_a$  causes on the velocity profile. Molecules of fluid can't move easily without more energy.
- It is evident from the **Fig. 7** that an increase in porous medium shape factor parameter  $S$  causes an enhancement on the velocity profile.
- It is noted that the velocity profile have a slight difference for varying values of porous medium shape factor parameter  $S$
- It should be noted that the value of  $S = 1$ , the profile of the velocity distribution seems to be a straight line.

### 5.1.2 For the microrotation profile graphed

**Figs. 8-10** are displayed to visualize the effect of various parameter on microrotation profile. the numerical calculations draw the following results:

- The impact of  $\beta$  and  $ha$  are portrayed in **Figs 8** and **9**. It is show that the higher values of  $\beta$  and  $ha$  enhances the microrotation profile.
- The increasing of  $S$  on microrotation profile  $g(\eta)$  increases as in **Fig. 10**.

### 5.1.3 For the temperature profile graphed

**Figs. 11-14** disclosed the impact of  $\beta, ha, S$  and  $B$  on the temperature profile.

- The behavior of  $\beta$  and  $ha$  on the temperature  $\theta(\eta)$  are depicted in **Figs. 11** and **12**. Here the effect of increasing  $\beta$  and  $ha$  that leads to an increase in temperature profile.
- The fluid temperature at increases with the increase of the heat generation parameter  $B$ , as shown in **Fig. 13**.
- Larger  $S$  reduces  $\theta(\eta)$  which results in argumentation of heat transfer at the wall as shown in **Fig. 14**.
- It is noted that the temperature profile has a sight difference for various values of  $S$ .

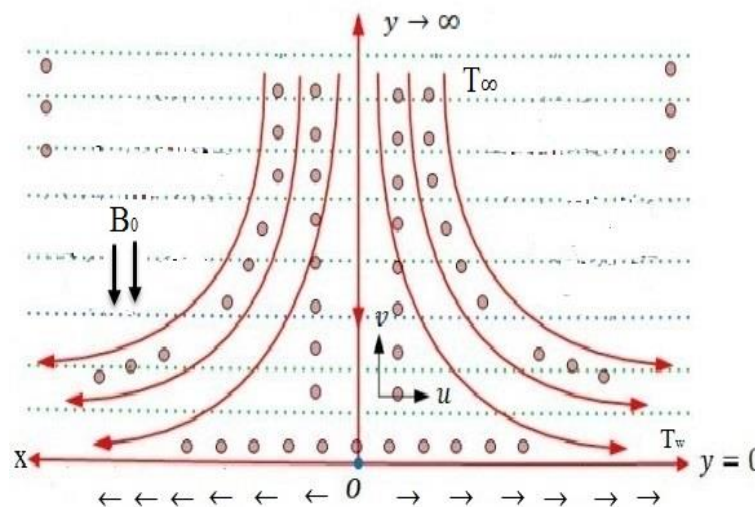


Fig 1: Physical flow diagram.

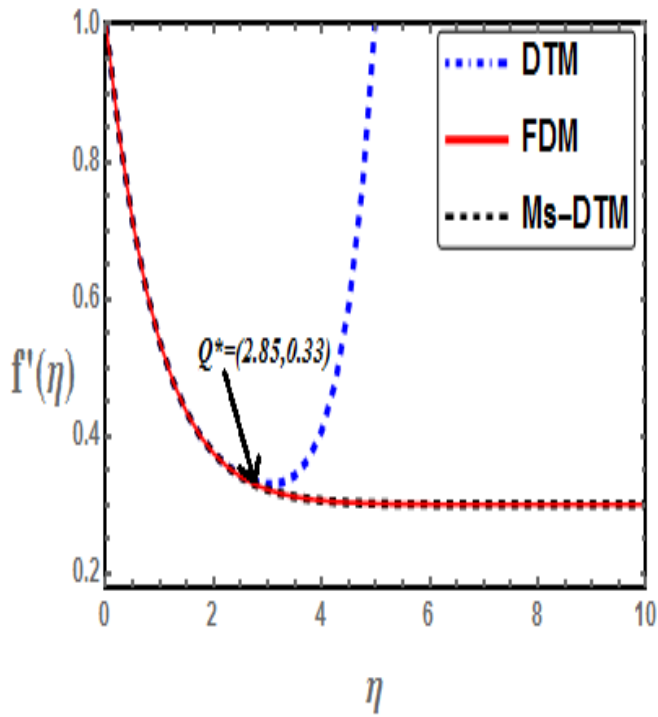


Fig 2. Behavior of velocity profile  $f(\eta)$  against  $\eta$  for values  $K = 0.1, ha = 0.3, Pr = 1, B = 0.7, \beta = 0.3, S = 0.1, Ec = 0.2, n = 1$ .

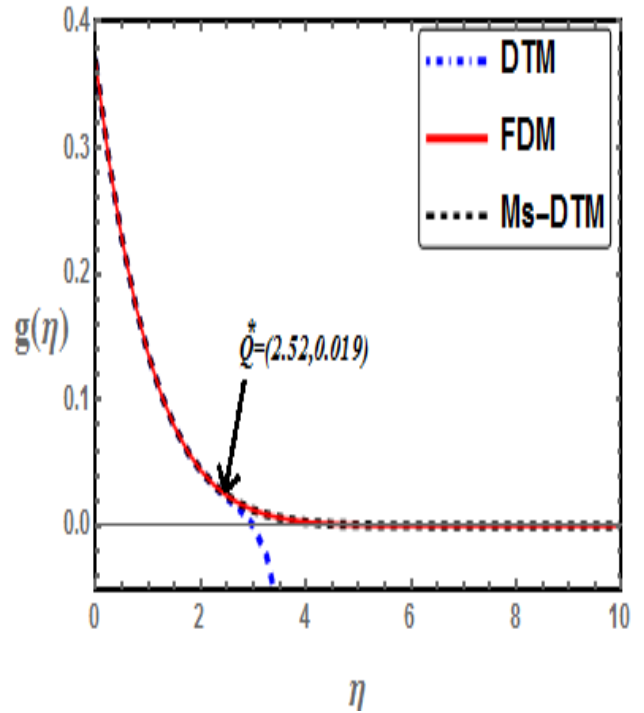


Fig 3. Behavior of microrotation profile  $g(\eta)$  against  $\eta$  for values  $K = 0.1, ha = 0.3, Pr = 1, B = 0.7, \beta = 0.3, S = 0.1, Ec = 0.2, n = 1$ .

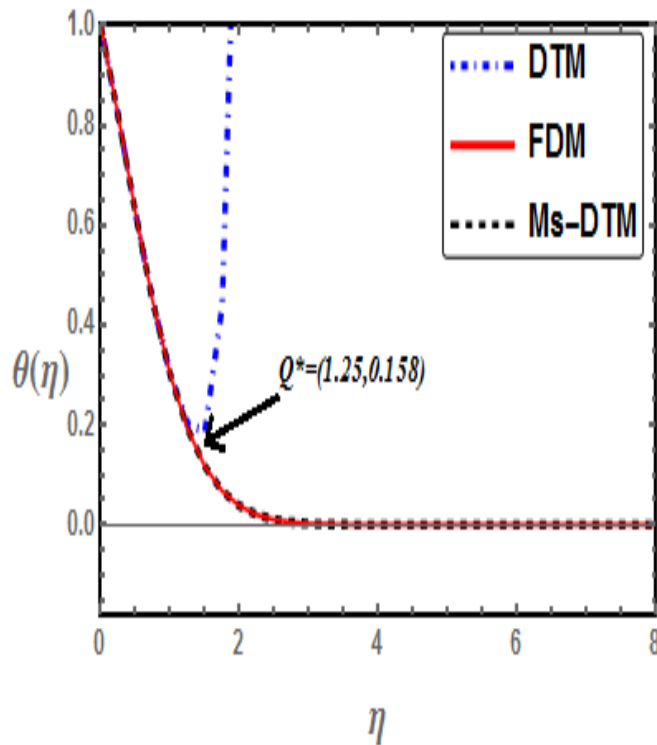


Fig 4. Behavior of temperature profile  $\theta(\eta)$  against  $\eta$  for values  $K = 0.1, ha = 0.3, Pr = 1, B = 0.7, \beta = 0.3, S = 0.1, Ec = 0.2, n = 1$ .

Table 1: Comparison between two numerical methods on a micropolar Casson fluid problem at  $K = 0.1, ha = 0.3, P_r = 1, B = 0.7, \beta = 0.3, S = 0.1, E_c = 0.2, n = 1$

$\eta$	$f'(\eta)$ FDM	$f'(\eta)$ Ms-Dtm	Error	$g(\eta)$ FDM	$g(\eta)$ Ms-Dtm	Error	$\theta(\eta)$ FDM	$\theta(\eta)$ Ms-Dtm	Error
0.	1.	1.	0.	0.367079	0.367091	0.0000123022	1.	1	0.
0.25	0.837335	0.837334	$-4.94622 \times 10^{-7}$	0.28978	0.289788	$8.23556 \times 10^{-8}$	0.819039	0.819043	$4.11781 \times 10^{-6}$
0.5	0.710593	0.710592	$-6.65241 \times 10^{-7}$	0.228899	0.228905	$5.41505 \times 10^{-8}$	0.62455	0.624558	$7.74406 \times 10^{-6}$
0.75	0.6123	0.612299	$-6.59041 \times 10^{-7}$	0.176179	0.176183	$3.49302 \times 10^{-8}$	0.446444	0.446454	0.0000100991
1.	0.536435	0.536435	$-5.67497 \times 10^{-7}$	0.135642	0.135645	$2.20787 \times 10^{-8}$	0.300934	0.300945	0.0000109063
1.25	0.478168	0.478168	$-4.45107 \times 10^{-7}$	0.103554	0.103555	$1.36594 \times 10^{-8}$	0.192244	0.192255	0.0000103407
1.5	0.433638	0.433637	$-3.22307 \times 10^{-7}$	0.0783986	0.0783994	$8.2637 \times 10^{-7}$	0.116874	0.116883	$8.8528 \times 10^{-6}$
1.75	0.399775	0.399774	$-2.14319 \times 10^{-7}$	0.0588694	0.0588699	$4.88704 \times 10^{-7}$	0.0678501	0.067857	$6.9568 \times 10^{-6}$
2.	0.374151	0.374151	$-1.27113 \times 10^{-7}$	0.0438522	0.0438525	$2.82734 \times 10^{-7}$	0.0377198	0.0377249	$5.07266 \times 10^{-6}$
2.25	0.354857	0.354857	$-6.13522 \times 10^{-8}$	0.0324121	0.0324122	$1.60454 \times 10^{-7}$	0.0201275	0.0201309	$3.4581 \times 10^{-6}$
2.5	0.3404	0.3404	$-1.49425 \times 10^{-8}$	0.0237758	0.0237759	$8.98017 \times 10^{-8}$	0.0103294	0.0103316	$2.21569 \times 10^{-6}$
2.75	0.329621	0.329621	$1.53931 \times 10^{-8}$	0.0173132	0.0173133	$4.99025 \times 10^{-8}$	0.00510738	0.00510872	$1.33877 \times 10^{-6}$
3.	0.321621	0.321621	$3.31827 \times 10^{-8}$	0.0125183	0.0125183	$2.75483 \times 10^{-8}$	0.00243723	0.00243799	$7.63733 \times 10^{-7}$
3.25	0.315712	0.315712	$4.17019 \times 10^{-8}$	0.00898955	0.00898957	$1.46496 \times 10^{-8}$	0.00112442	0.00112483	$4.10413 \times 10^{-7}$
3.5	0.311368	0.311368	$4.37404 \times 10^{-8}$	0.00641309	0.00641309	$6.43692 \times 10^{-9}$	0.000502499	0.000502705	$2.05802 \times 10^{-7}$
3.75	0.308189	0.308189	$4.15324 \times 10^{-8}$	0.00454608	0.00454608	$2.24776 \times 10^{-10}$	0.000218034	0.000218128	$9.36455 \times 10^{-8}$
4.	0.305873	0.305873	$3.6778 \times 10^{-8}$	0.00320295	0.00320295	$-5.41458 \times 10^{-9}$	0.0000921164	0.0000921517	$3.5282 \times 10^{-8}$
4.25	0.304194	0.304194	$3.07117 \times 10^{-8}$	0.00224341	0.0022434	$-1.11866 \times 10^{-8}$	0.0000380308	0.0000380372	$6.39963 \times 10^{-9}$
4.5	0.302982	0.302982	$2.41869 \times 10^{-8}$	0.00156245	0.00156244	$-1.74088 \times 10^{-8}$	0.0000154129	0.0000154057	$-7.19174 \times 10^{-9}$
4.75	0.302111	0.302111	$1.77615 \times 10^{-8}$	0.00108228	0.00108225	$-2.42113 \times 10^{-8}$	$6.16575 \times 10^{-6}$	$6.1525 \times 10^{-6}$	$-1.32503 \times 10^{-8}$
5.	0.301488	0.301488	$1.17737 \times 10^{-8}$	0.000745743	0.000745711	$-3.16494 \times 10^{-8}$	$2.45041 \times 10^{-6}$	$2.43464 \times 10^{-6}$	$-1.57746 \times 10^{-8}$
5.25	0.301044	0.301044	$6.40675 \times 10^{-9}$	0.000511254	0.000511214	$-3.97634 \times 10^{-8}$	$9.74224 \times 10^{-7}$	$9.57507 \times 10^{-7}$	$-1.67169 \times 10^{-8}$
5.5	0.30073	0.30073	$1.73957 \times 10^{-9}$	0.00034878	0.000348732	$-4.86052 \times 10^{-8}$	$3.90058 \times 10^{-7}$	$3.73075 \times 10^{-7}$	$-1.6983 \times 10^{-8}$
5.75	0.300507	0.300507	$-2.21407 \times 10^{-9}$	0.000236809	0.000236751	$-6.82483 \times 10^{-8}$	$1.5811 \times 10^{-7}$	$1.41135 \times 10^{-7}$	$-1.69742 \times 10^{-8}$
6.	0.300351	0.300351	$-5.47732 \times 10^{-9}$	0.00016004	0.000159972	$-6.87883 \times 10^{-8}$	$6.50826 \times 10^{-8}$	$4.82223 \times 10^{-8}$	$-1.68603 \times 10^{-8}$
6.25	0.300242	0.300242	$-8.09021 \times 10^{-9}$	0.000107668	0.000107588	$-8.03399 \times 10^{-8}$	$2.72147 \times 10^{-8}$	$1.05044 \times 10^{-8}$	$-1.67103 \times 10^{-8}$
6.5	0.300166	0.300166	$-1.00963 \times 10^{-8}$	0.0000721112	0.0000720182	$-9.30328 \times 10^{-8}$	$1.15374 \times 10^{-8}$	$-5.01347 \times 10^{-9}$	$-1.65508 \times 10^{-8}$
6.75	0.300113	0.300113	$-1.1534 \times 10^{-8}$	0.000048083	0.0000479759	$-1.07008 \times 10^{-7}$	$4.94152 \times 10^{-9}$	$-1.14505 \times 10^{-8}$	$-1.6392 \times 10^{-8}$
7.	0.300077	0.300077	$-1.24318 \times 10^{-8}$	0.0000319188	0.0000317964	$-1.22416 \times 10^{-7}$	$2.12976 \times 10^{-9}$	$-1.41075 \times 10^{-8}$	$-1.62373 \times 10^{-8}$
7.25	0.300052	0.300052	$-1.28054 \times 10^{-8}$	0.0000210928	0.0000209534	$-1.39414 \times 10^{-7}$	$9.20213 \times 10^{-10}$	$-1.51674 \times 10^{-8}$	$-1.60876 \times 10^{-8}$
7.5	0.300035	0.300035	$-1.26564 \times 10^{-8}$	0.000013873	0.0000137149	$-1.58165 \times 10^{-7}$	$3.97364 \times 10^{-10}$	$-1.55458 \times 10^{-8}$	$-1.59431 \times 10^{-8}$
7.75	0.300023	0.300023	$-1.19726 \times 10^{-8}$	$9.07789 \times 10^{-6}$	$8.89905 \times 10^{-6}$	$-1.78839 \times 10^{-7}$	$1.71081 \times 10^{-10}$	$-1.56326 \times 10^{-8}$	$-1.58037 \times 10^{-8}$
8.	0.300016	0.300015	$-1.07283 \times 10^{-8}$	$5.90549 \times 10^{-6}$	$5.70388 \times 10^{-6}$	$-2.01612 \times 10^{-7}$	$7.33117 \times 10^{-11}$	$-1.55958 \times 10^{-8}$	$-1.56691 \times 10^{-8}$
8.25	0.30001	0.30001	$-8.88447 \times 10^{-9}$	$3.81402 \times 10^{-6}$	$3.58735 \times 10^{-6}$	$-2.26667 \times 10^{-7}$	$3.12271 \times 10^{-11}$	$-1.55078 \times 10^{-8}$	$-1.5539 \times 10^{-8}$
8.5	0.300007	0.300007	$-6.39011 \times 10^{-9}$	$2.43915 \times 10^{-6}$	$2.18496 \times 10^{-6}$	$-2.54193 \times 10^{-7}$	$1.32041 \times 10^{-11}$	$-1.54 \times 10^{-8}$	$-1.54132 \times 10^{-8}$
8.75	0.300004	0.300004	$-3.18245 \times 10^{-9}$	$1.53698 \times 10^{-6}$	$1.2526 \times 10^{-6}$	$-2.84389 \times 10^{-7}$	$5.53081 \times 10^{-12}$	$-1.5286 \times 10^{-8}$	$-1.52915 \times 10^{-8}$
9.	0.300003	0.300003	$8.12329 \times 10^{-10}$	$9.4496 \times 10^{-7}$	$6.27499 \times 10^{-7}$	$-3.17461 \times 10^{-7}$	$2.28357 \times 10^{-12}$	$-1.51713 \times 10^{-8}$	$-1.51735 \times 10^{-8}$
9.25	0.300002	0.300002	$5.67871 \times 10^{-9}$	$5.55196 \times 10^{-7}$	$2.0157 \times 10^{-7}$	$-3.53626 \times 10^{-7}$	$9.16829 \times 10^{-13}$	$-1.50583 \times 10^{-8}$	$-1.50592 \times 10^{-8}$
9.5	0.300001	0.300001	$1.15115 \times 10^{-8}$	$2.96387 \times 10^{-7}$	$-9.67227 \times 10^{-8}$	$-3.9311 \times 10^{-7}$	$3.43543 \times 10^{-13}$	$-1.4948 \times 10^{-8}$	$-1.49483 \times 10^{-8}$
9.75	0.3	0.3	$1.84159 \times 10^{-8}$	$1.21589 \times 10^{-7}$	$-3.14561 \times 10^{-7}$	$-4.36149 \times 10^{-7}$	$1.02666 \times 10^{-13}$	$-1.48405 \times 10^{-8}$	$-1.48406 \times 10^{-8}$
10.	0.3	0.3	$2.65071 \times 10^{-8}$	0.	$-4.82992 \times 10^{-7}$	$-4.82992 \times 10^{-7}$	0.	$-1.4736 \times 10^{-8}$	$-1.4736 \times 10^{-8}$

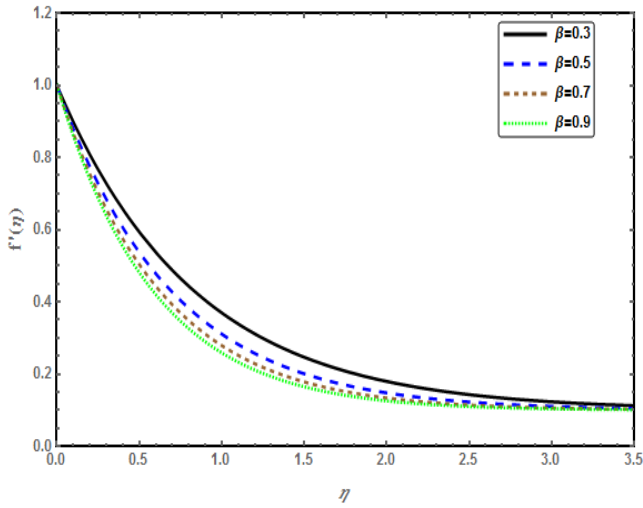


Fig 5. Behavior of velocity profile  $f'(\eta)$  against  $\eta$  for several values  $K = 0.1, ha = 0.3, Pr = 1, B = 0.7, S = 0.1, Ec = 0.2, n = 1$ .

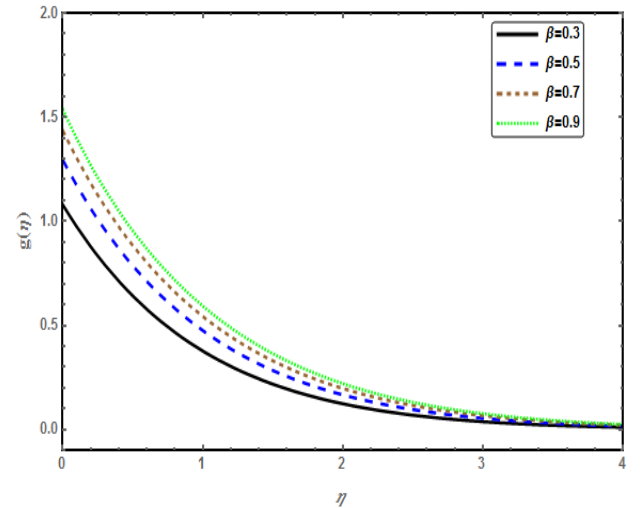


Fig 8. Behavior of microrotation profile  $g(\eta)$  against  $\eta$  for several values  $K = 0.1, ha = 0.3, Pr = 1, s = 0.2, B = 0.7, Ec = 0.2, n = 1$ .

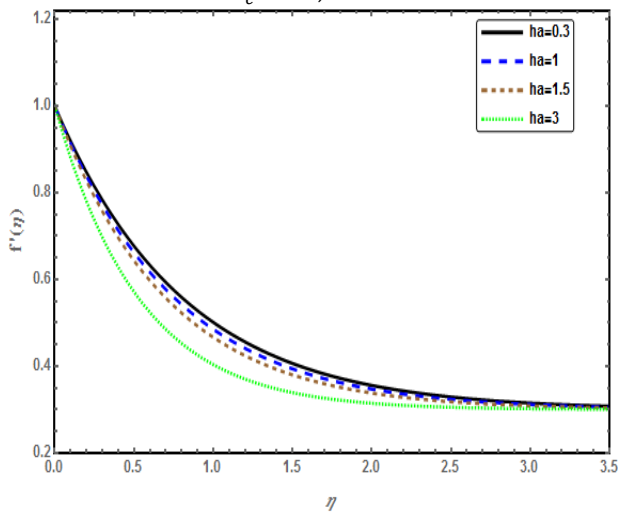


Fig 6. Behavior of velocity profile  $f'(\eta)$  against  $\eta$  for several values  $K = 0.1, Pr = 1, \beta = 0.2, B = 0.7, S = 0.1, Ec = 0.2, n = 1$ .

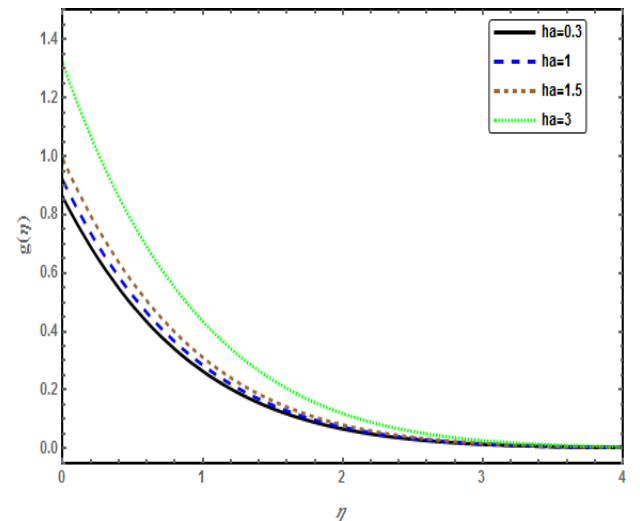


Fig 9. Behavior of microrotation profile  $g(\eta)$  against  $\eta$  for several values  $K = 0.1, s = 0.2, Pr = 1, \beta = 0.2, B = 0.7, Ec = 0.2, n = 1$ .

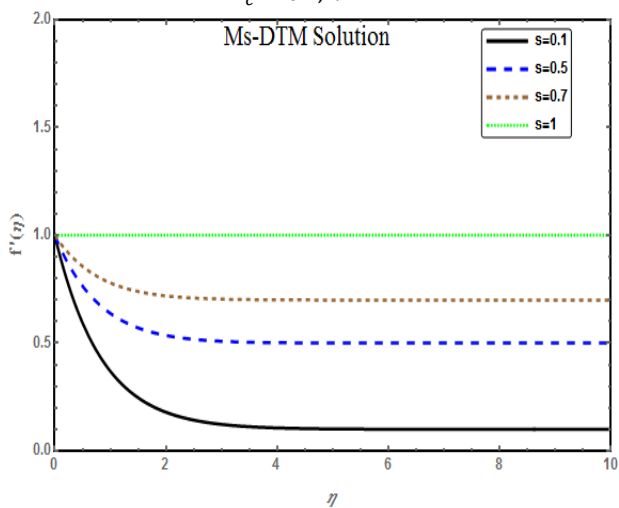


Fig 7. Behavior of velocity profile  $f'(\eta)$  against  $\eta$  for several values  $K = 0.1, ha = 0.3, Pr = 1, \beta = 0.2, B = 0.7, Ec = 0.2, n = 1$ .

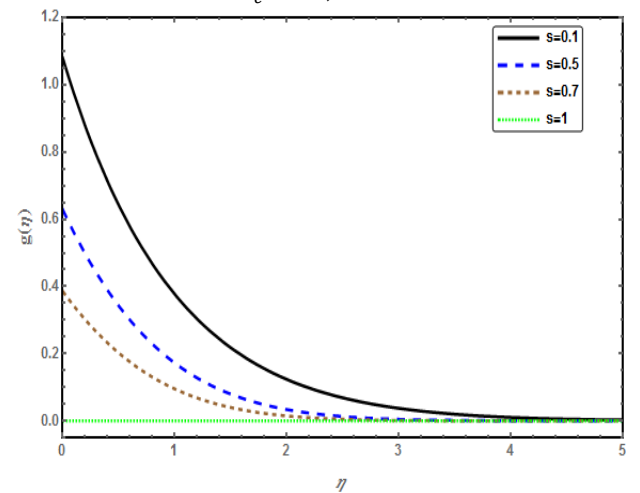


Fig 10. Behavior of microrotation profile  $g(\eta)$  against  $\eta$  for several values  $K = 0.1, ha = 0.3, Pr = 1, \beta = 0.2, B = 0.7, Ec = 0.2, n = 1$ .

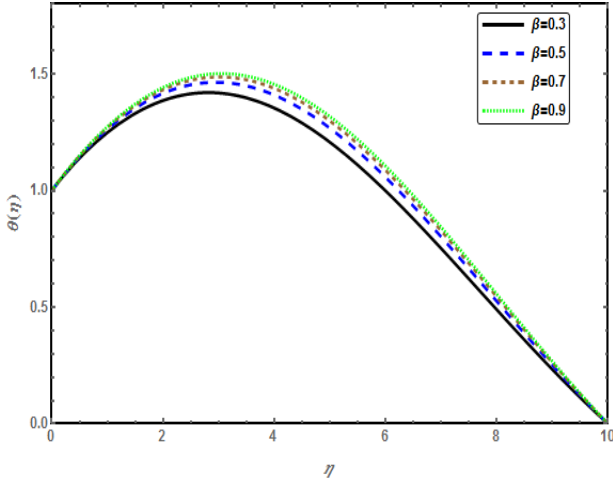


Fig 11. Behavior of temperature profile  $\theta(\eta)$  against  $\eta$  for several values  $K = 0.1, ha = 0.3, P_r = 1, s = 0.2, B = 0.7, E_c = 0.2, n = 1$ .

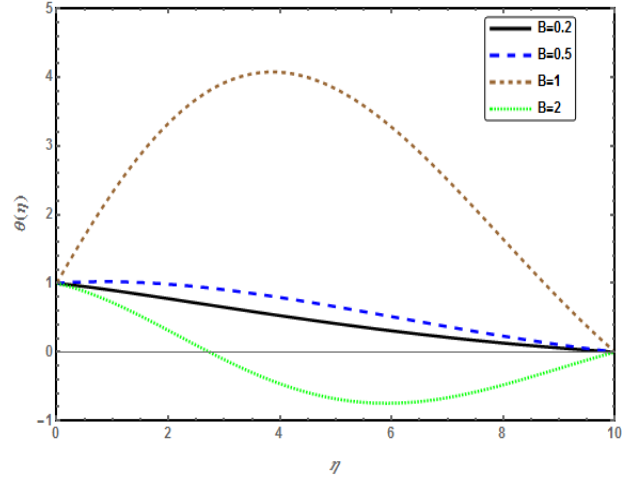


Fig 13. Behavior of temperature profile  $\theta(\eta)$  against  $\eta$  for several values  $K = 0.1, ha = 0.3, P_r = 1, \beta = 0.2, s = 0.1, E_c = 0.2, n = 1$ .

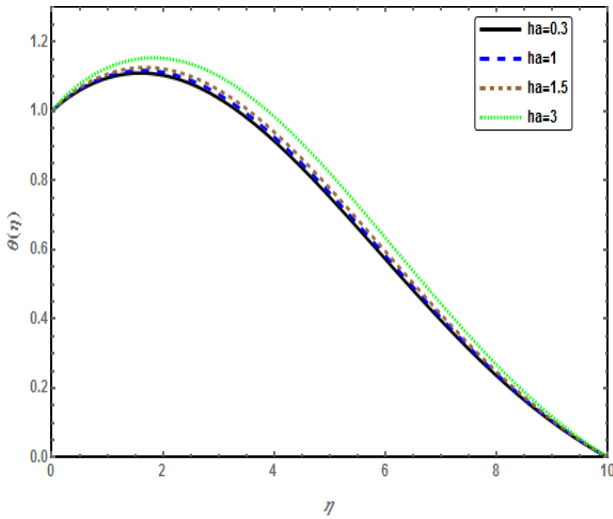


Fig 12. Behavior of temperature profile  $\theta(\eta)$  against  $\eta$  for several values  $K = 0.1, s = 0.2, P_r = 1, \beta = 0.2, B = 0.7, E_c = 0.2, n = 1$ .

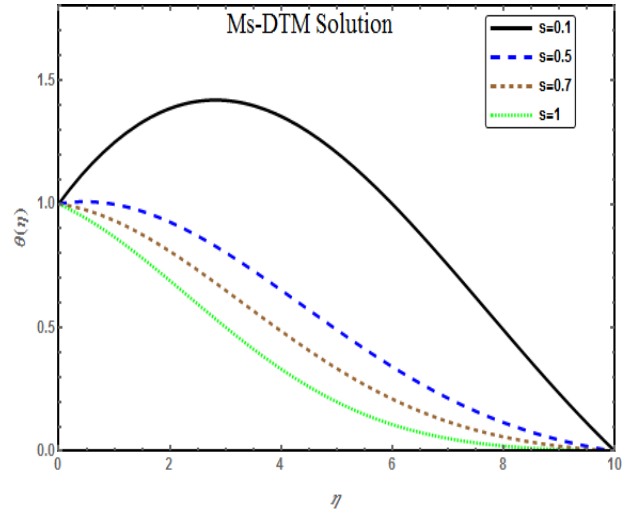


Fig 14. Behavior of temperature profile  $\theta(\eta)$  against  $\eta$  for several values  $K = 0.1, ha = 0.3, P_r = 1, \beta = 0.2, B = 0.7, E_c = 0.2, n = 1$ .

## 6 Concluding remarks

The current paper investigates an incompressible micropolar Casson fluid over a stretching surface. Porous medium and heat generation are taken into consideration. The governing equations of motion are analytically solved through Ms-DTM to obtain the distribution of velocity, microrotation and temperature. Ms-DTM are applicable to nonlinear models such as micropolar Casson fluid models which is more complicated and have a higher degree of non-linearity, in a direct way without using linearization or restrictive assumptions. The velocity, microrotation in space-time domain and temperature are obtained for different times and for various values of material parameters using a Ms-DTM. The investigation draws the following concluding remarks.

- The influences of  $\beta$  and  $ha$  on  $f'(\eta)$  are similar in a qualitative sense.
- Temperature and microrotation are reduced for higher values of  $S$ .
- At  $S = 1$ , it is seen that no variation for the velocity and microrotation parameter profiles. Therefore they graphed a horizontal straight line.

- The advantage of the Ms-DTM is to make a linearization for the nonlinear system. Therefore, away from any other methods, we can easily solve the problem.
- An accuracy comparison is made between the methods of FDM and Ms-DTM. This comparison shows that the error between them is efficiently small.

## References

- [1] A.C. Eringen, Theory of Micropolar Fluids, Journal of Mathematical Mechanics, New York, **16** (1966) 1–18.
- [2] N. Ali and T. Hayat, Peristaltic flow of a micropolar fluid in an asymmetric channel. Computer and Applied Math, **55** (2008), 589–608.
- [3] S. Ahmad, M. Ashraf and K.S. Sayed, Effects of thermal radiation on MHD axisymmetric stagnation point flow and heat transfer of a micropolar fluid over a shrinking sheet, World Applied Sciences Journal, **15** (2011) 835-848.
- [4] N.T. Eldabe and M.Y. Abou-zeid, Magnetohydrodynamic peristaltic flow with heat and mass transfer of micropolar biviscosity fluid through a porous medium between two Co-Axial Tubes, Arab Journal Science Engineering, **39** (2014) 5045–5062.
- [5] M. Nazeer, N. Ali and T. Javed, Numerical simulation of MHD flow of micropolar fluid inside a porous inclined cavity with uniform and non-uniform heated bottom wall, Can J Phys. **96** (6), 576-593, 2017.
- [6] S. R. Mishra, I. Khan, Q.M. Al-mdallal and T. Asifa, Free convective micropolar fluid flow and heat transfer over a shrinking sheet with heat source, Case Studies in Thermal Engineering, **11**, 113-119, 2018.
- [7] N. Ali, M. Nazeer, T. Javed and M. A. Siddiqui, Buoyancy driven cavity flow of a micropolar fluid with variably heated bottom wall, Heat Trans. Res., **49**(5), 457-481, 2018.
- [8] M. Nazeer, N. Ali and T. Javed, Numerical simulations of MHD forced convection flow of micropolar fluid inside a right angle triangular cavity saturated with porous medium: Effects of vertical moving wall, Can J Phys., **97**, 1-25, 2018.
- [9] N. A. Khan, S. Khan, A. Ara, Flow of micropolar fluid over an off centred rotating disk with modified Darcy's law, Propulsion and Power Research, **6**, 285-295, 2017.
- [10] N. A. Khan, F. Naz, F. Sultan, Entropy generation analysis and effects of slip conditions on micropolar fluid flow due to a rotating disk, Open Engineering **7**(1), 185–198, 2017.
- [11] M., Asad, C. Bin, G. Abuzar, Hydromagnetic Hiemenz flow of micropolar fluid over a nonlinearly stretching/shrinking sheet: Dual solutions by using Chebyshev Spectral Newton Iterative Scheme. Journal of Magnetism and Magnetic Materials, **416**, 329-334.
- [12] Z. Shah, S. Islam, T. Gul, E. Bonyah and M. A. Khan, The electrical MHD and Hall current impact on micropolar nanofluid flow between rotating parallel plates, **9**, 1201-1214, 2018.

- [13] N. T. M. El-dabe, G. M. Moatimeid, M.A .Hassan and E.S.Ashour, Heat and Mass transfer of magnetohydrodynamic pulsatile Flow of Casson Fluid with couple stress through porous medium, *International Journal of Current Engineering and Technology*, **6** (2016) 1414-1421.
- [14] Kh. S. Mekheimer, Nonlinear peristaltic transport through a porous medium in an inclined planar channel. *Journal of Porous Media*, **6** (2003) 190–202.
- [15] J. Zueco and S. Ahmed, Combined heat and mass transfer by mixed convection MHD flow along a porous plate with chemical reaction in presence of heat source, *Applied Mathematics and Mechanics*, **31**(2010), 1217–1230.
- [16] N. T. M. El-dabe, G. M. Moatimid, M. A. Hassan and D. R. Mostapha, Effect of partial slip on peristaltic flow of a Sisko fluid with mild stenosis through a porous medium, *Applied Mathematics and Information Sciences*, **10** (2016) 673-687.
- [17] G. V. Vinogradov and A. Y. Malkin, *Rheology of Polymers*, Mir Publisher, Moscow (1979) .
- [18] Z. Mehmood, R. Mehmood, and Z. Iqbal, Numerical investigation of micropolar Casson fluid over a stretching sheet with internal heating, *Communication Theory of Physics*, **67** (2017) 443–448.
- [19] Z. Iqbal, R. Mehmood, E. Azhara and Z. Mehmood, Impact of inclined magnetic field on micropolar Casson fluid using Keller box algorithm, *The European Physical Journal Plus*, **15** (2017)132-175.
- [20] K. Hiemenz, Die Grenzschicht neinem in den gleichformigen flussigkeitsstrom eingetauchten geraden Kreiszyylinder, *Dingler’s Polytech Journal*, 326 (1911) 321–410.
- [21] S.Shateyi and OD. Makinde, Hydromagnetic stagnation-point flow towards a radially stretching convectively heated disk. *Mathematical Problems in Engineering* (2013).
- [22] K. Bhattacharyy, S. Mukhopadhyay and G. C. Layek, Slip effects on boundary layer stagnation-point flow and heat transfer towards a shrinking sheet, *International Journal physics of Heat and Mass Transfer*, **54**(2011)308–13.
- [23] S. S. Motsa and K.Y.S. Shateyi, A new numerical solution of Maxwell fluid over a shrinking sheet in the region of a stagnation point, *Mathematical Problems in Engineering* (2012).
- [24] T. Javed and A. Ghaffari, Numerical study of non-Newtonian Maxwell fluid in the region of oblique stagnation point flow over a stretching sheet, *Journal of Mechanics* 32 (2), 175-184.
- [25] I. Mustafa, T. Javed and A. Ghaffari, Heat transfer in MHD stagnation point flow of a ferrofluid over a stretchable rotating disk, *Journal of Molecular Liquids* 219, 526-532.
- [26] A. Ghaffari, T. Javed and F. Labropulu, Heat transfer analysis of unsteady oblique stagnation point flow of elastico- viscous fluid due to sinusoidal wall temperature over an oscillating-stretching surface: A numerical approach, *Journal of Molecular Liquids* 219, 748-755.
- [27] Y. Tasaka, Y. Kudoh, Y. Takeda and T. Yanagisawa, Experimental investigation of natural convection induced by internal heat generation, *Journal of Physics: Conference series*, **14** (2005) 168–79.
- [28] J. C. Crepeau and R. Clarksean, Similarity solutions of natural convection with internal heat generation, *Trans ASME, Journal of Heat Transfer*, **119** (1997) 184–5.

- [29] A. M.Salem and MA.El-Aziz, MHD-mixed convection and mass transfer from a vertical stretching sheet with diffusion of chemically reactive species and space or temperature dependent heat source, *Canadian Journal of Physics*, **85** (2007)359–73.
- [30] A. M.Salem and MA.El-Aziz, Effect of Hall currents and chemical reaction on hydromagnetic flow of a stretching vertical surface with internal heat generation/absorption, *Applied Mathematical Modelling*, **32** (2008)1236–1254.
- [31] S. Muhammad, G. Ali,Z. Shah, S. Islam and S. A. Hussain, The Rotating Flow of Magneto Hydrodynamic Carbon Nanotubes over a Stretching Sheet with the Impact of Non-Linear Thermal Radiation and Heat Generation/Absorption, *Applied Sciences*, 8(4), **2018**, 482.
- [32] A. Ghaffari, Enhancement of heat transfer in elastico-viscous fluid due to nanoparticles, where the fluid is impinging obliquely to the stretchable surface: A numerical study. *Applications & Applied Mathematics*, 11(1) 251-265.
- [33] Z. Shah, T. Gul, S. Islam, M. A. Khan, E. Bonyah, F. Hussain, S. Mukhtar, M. Ullah, Three dimensional third grade nanofluid flow in a rotating system between parallel plates with Brownian motion and thermophoresis effects, *Results in Physics*, 10, 36-45, 2018.
- [34] Z. Shah and S. Islam, Effects of hall current on steady three dimensional non-newtonian nanofluid in a rotating frame with brownian motion and thermophoresis effects, *Journal of Engineering Technology*, 6, 280-296, 2017.
- [35] N. Ali, F.Nazeer, M. Nazeer, Flow and heat transfer analysis of Eyring-powell fluid in a pipe, *Zeitschrift für Naturforschung A (ZNA)*, 73 (3), 265–274. doi.org/10.1515/zna-2017-0435.
- [36] M. Ishaq, G. Ali, Z. Shah, S. Islam and S. Muhammad, Entropy Generation on Nanofluid Thin Film Flow of Eyring–Powell Fluid with Thermal Radiation and MHD Effect on an Unsteady Porous Stretching Sheet, *Entropy*, 20, 412-436, 2018.
- [37] S. Nasir, S. Islam, T. Gul, Z. Shah, M. A. Khan, W. Khan, A. Z. Khan and S. Khan, Three-dimensional rotating flow of MHD single wall carbon nanotubes over a stretching sheet in presence of thermal radiation, *Applied Nanoscience* 8, 1361–1378, 2018.
- [38] Z. M. Odibat, C.Bertelle, M.A. Aziz-Alaoui and H.E.G. Duchamp, A multistep differential transform method and application to non-chaotic or chaotic systems, *Computers and Mathematics with Applications*, **59** (2010) 1462– 1472.
- [39] R.A. Zait, A.A. El-Shehki and N.M. Abdo, Statistical measures approximations for the Gaussian part of the stochastic nonlinear damped Duffing oscillator solution process under the application of Wiener Hermite expansion linked by the multi-step differential transformed method, *Journal of the Egyptian Mathematical Society*, **24**(2016) 1–12.
- [40] R.Courant, K.O.Friedrichs and H. Lewy, Uber die partiellen differenzgleichungen der mathematischen physik, *Mathematische Annalen*, **100** (1928) 32–74.
- [41] R.J. LeVeque, *Finite Difference Methods for Ordinary and Partial Differential Equations*, Society for Industrial and Applied Mathematics, Washington, (2007).
- [42] V. Thomee, From finite differences to finite elements a short history of numerical analysis of partial differential equations, *Journal of Computational and Applied Mathematics*, **128** (2001) 1–54.